Proceedings of the ASME 2015 Internal Combustion Engine Division Fall Technical Conference
ICEF2015
November 8-11, 2015, Houston, TX, USA

ICEF2015-1173

FAST COMPUTATION OF COMBUSTION PHASING AND ITS INFLUENCE ON CLASSIFYING RANDOM OR DETERMINISTIC PATTERNS

Huan Lian*, Jason Martz, Niket Prakash, Anna Stefanopoulou
Department of Mechanical Engineering
University of Michigan
Ann Arbor, Michigan 48109
Email: hlian@umich.edu

ABSTRACT

The classification between a sequence of highly variable combustion events that have an underlying deterministic pattern and a sequence of combustion events with similar level of variability but random characteristics is important for control of combustion phasing. In the case of high cyclic variation (CV) with underlying deterministic patterns, it is possible to apply closed loop combustion control on a cyclic-basis with a fixed mean value, such as injection timing in homogeneous charge compression ignition (HCCI) or spark timing in spark ignition (SI) applications, to contract the CV. In the case of a random distribution, the high CV can be avoided by shifting operating conditions away from the unstable region via advancing or retarding the injection timing or the spark timing in the mean-sense.

Therefore, the focus of this paper is on the various methods of computing CA50 for analysing and classifying cycle-to-cycle variability. The assumptions made to establish fast and possibly on-line methods can alter the distribution of the calculated parameters from cycle-to-cycle, possibly leading to incorrect pattern interpretation and improper control action.

Finally, we apply a statistical technique named "permutation entropy" for the first time on classifying combustion patterns in HCCI and SI engine for varying operating condition. Then the various fast methods for computing CA50 feed the two statistical methods, permutation and the Shannon entropy, and their differences and similarities are highlighted.

*Address all correspondence to this author.

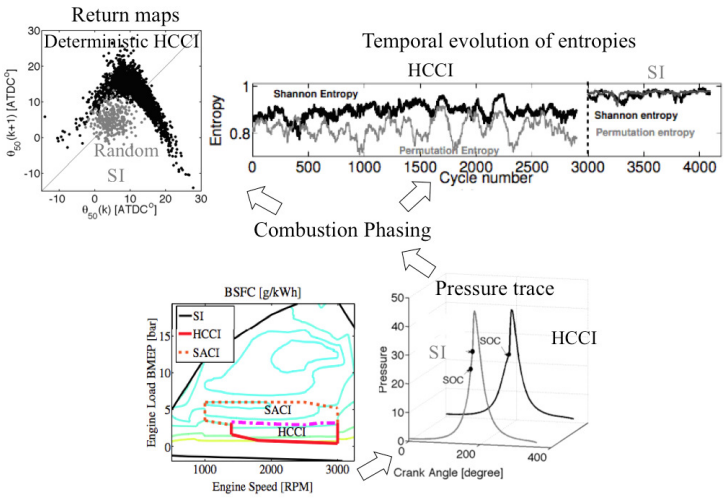

Figure 1. Scope of the current work (Engine map from reference [1])

NOMENCLATURE

P	Pressure
V	Volume
γ	Polytropic Exponent
n	Polytropic Coefficient
x_b	Mass Fraction Burned
$CA50$	Crank Angle of 50% Mass Fraction Burned
Q_{ch}	Chemical Energy
$Q_{apparent}$	Apparent Heat Release

θ	Crank Angle Degree
m_c	In-cylinder Charge Mass
c_v	Constant Volume Specific Heat
T	Temperature
Q_{ht}	Heat Transfer
$\overline{R}$	Universal Gas Constant
M	Molar Mass
A/F	Air Fuel Ratio
$\overline{h}$	Heat Transfer Coefficient
subscript u	Unburned
subscript b	Burned
subscript σ	Property At Start Of Combustion
subscript f	Property At End Of Combustion
Q_{hv}	Lower Heating Value Of The Fuel
A	Combustion Chamber Surface Area
ω	Crank Angle Degrees Per Unit Time
T_w	Cylinder Wall Temperature
H_s	modified Shannon entropy
H_p	permutation entropy
H_n	Normalized permutation entropy
p_k	Probability of a Sequence

1. INTRODUCTION

Control of combustion process on a cycle-to-cycle basis can improve fuel economy and emission performance. The characteristics of combustion process represented by combustion phasing could be random [2] or deterministic [3, 4], and would lead to a different control strategy aiming to contract the CV. In the case of high cyclic variation with underlying deterministic patterns, it is possible to apply closed loop combustion control of certain variable on a cycle-basis with a fixed mean value, such as injection timing in HCCI engine or spark timing in SI engine, to contract the CV. In the case of a random distribution, the high CV should be avoided by shifting operating conditions via advancing or retarding the injection timing or the spark timing in the mean-sense.

Real time heat release can be used with statistical methods for on-line quantification of combustion process variations as random or deterministic. However, errors within these fast heat release analyses can bias sequence statistics and lead to the incorrect classification of combustion variations as random or deterministic, potentially leading to improper control action. In the current work, we compare the influence of several fast heat release methods on the statistics of deterministic, high CV HCCI combustion and SI combustion where the CV is random in nature.

The paper is organised as follows: In Section 2, three fast computational methods for the determination of combustion phasing are briefly described. In Section 3, cyclic variation is quantified with return maps, the modified Shannon entropy and symbol statistics. The impact of each combustion phasing estimation method on the quantification of cyclic variation is assessed through comparison with the baseline detailed heat release analysis [5]. Section 4 introduces a diagnostic technique based on the permutation entropy to classify if SI and HCCI combustion process are deterministic or random, which is necessary for choosing the optimal control strategy. Comparisons with modified Shannon entropy is also included. Fig. 1 summarizes the scope of the current work.

2. Estimation of Combustion Phasing

Three fast combustion phasing estimation methods have been evaluated for HCCI and SI combustion phasing: Fast, single zone heat release with a constant ratio of specific heats [2], Rasseweiler and Withrow's method based on the assumption of isentropic compression and expansion [2] and Marvin's graphic method [6]. The methods were evaluated offline against detailed heat release analysis which estimates burned gas properties with chemical equilibrium and a routine for the prediction of trapped residual mass [5].

2.1. Experimental Setup

SI and HCCI combustion experiments were performed in a prototype modified four-cylinder 2.0 *L* SI engine, based on the GM Ecotec, running on Tier-II certification gasoline fuel. The compression ratio was 11.7, the bore and stroke were 88 *mm*, and the connecting rod length was 146 *mm*. The engine was designed for running multiple modes of combustion such as a HCCI, SACI, and SI. The important features of the engine were dual-lift valvetrain with dual-independent cam phasers, external exhaust gas recirculation(eEGR), spray-guided direct and port fuel injection, and in-cylinder pressure sensing. The data presented here for SI combustion was operated close to stoichiometry, with direct injection, and with low cam lift intake and exhaust profile. Negative valve overlap was utilized to trap up to approximately 40% internal residual, while a high-pressure EGR system provides cooled external residual gas [7, 8]. For HCCI combustion, the data was taken from experiments at constant speed of 2,000 rpm, with fuel injection at 60 deg after top dead center NVO. The chosen condition was diluted and lean with approximately 50% residual gas and air-fuel equivalence ratio of 1.3 to 1.4 [9].

2.2. Marvin's Method

Marvin [6] proposed a graphical method with a logarithmic P-V diagram based on the assumption that both compression and expansion processes follow a polytropic relation:

$$PV^{\gamma} = constant. \tag{1}$$

Marvin's method is illustrated in Fig. 2. Constant volume combustion was assumed to follow the polytropic compression process with the pressure rise shown between point b and d. The the mass fraction burned at point c on the line $b-d$ can be estimated as:

$$x_b = \frac{P_c - P_b}{P_d - P_c}. \tag{2}$$

By drawing a line $c-c'$ from point c parallel to the polytropic compression slope that intersects with the actual P-V diagram at c', a combination of in-cylinder pressure and volume is defined from the intersection point. The corresponding combustion phasing crank angle can be uniquely calculated from the combination of pressure and volume.

A natural question of this technique, is the resolution in defining the intersection point and combustion phasing calculation. We have found that $1/10$ crank angle is a reasonable measurement resolution for SI combustion applications, which has been adopted for all the results in the current work. In the case with poor measurement resolution, it is recommended to interpolate the pressure data with a cubic interpolation method to ensure estimation accuracy.

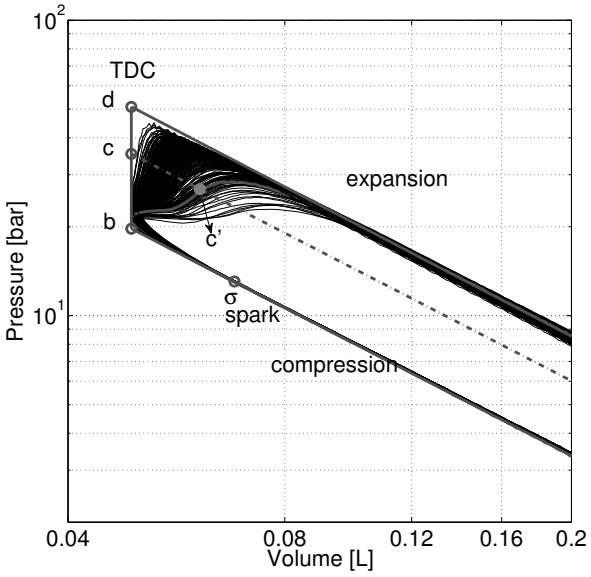

Figure 2. Marvin's graphical method for estimating combustion phasing of SI combustion, with 42% internal EGR fraction, spark timing 38 deg bTDC, 298 cycles

2.3. Rasseweiler and Withrow's Method

Another well-known method to estimate combustion phasing was proposed by Rassweiler and Withrow [10] who correlated pressure rise with flame photographs. The analysis assumes that unburned gas with a volume of V_u has been compressed polytropically through the expansion of the charge as it is consumed by the flame front, thus the unburned gas volume $V_{u,\sigma}$ at the start of combustion can be expressed as:

$$V_{u,\sigma} = V_u \left(P/P_\sigma\right)^{1/n}, \tag{3}$$

where P is the crank-angle-resolved in-cylinder pressure and P_σ is the pressure at the start of combustion, defined as the time of spark timing for SI and intake valve closing (IVC) for HCCI combustion.

Similarly the burnt gas volume $V_{b,f}$ at the end of combustion can be expressed in Eq. 4, where the end of combustion is arbitrarily defined. In the current work on SI combustion, we define the end of combustion around the crank angle where the $P-V$ diagram converges to the polytropic expansion phase as shown in Fig. 2. For HCCI combustion, it is difficult to identify the crank angle where the logarithmic $P-V$ diagram converges to the polytropic expansion phase, due to the presence of slow burning cycles. The end of combustion (EOC) is defined approximately 30^o after top dead center, where combustion ends in most of the cycles. It should be noted that the arbitrary choice of the end of combustion is the major factor responsible for the inaccuracy of this method.

$$V_{b,f} = V_b \left(P/P_f\right)^{1/n}. \tag{4}$$

The mass fraction burned x_b can be approximated with the unburned gas volume consumed by the flame front as:

$$x_b = 1 - \frac{V_{u,\sigma}}{V_\sigma}. \tag{5}$$

Combining Eq. 3-5 and considering volume conservation $V = V_u + V_b$, the mass fraction burnt x_b is then derived as:

$$x_b = \frac{P^{1/n}V - P_\sigma^{1/n}V_\sigma}{P_f^{1/n}V_f - P_\sigma^{1/n}V_\sigma}. \tag{6}$$

The polytropic exponent n has been used as an averaged value of compression and expansion processes.

The combustion phasing crank angle is calculated from the interpolation of the mass fraction burned x_b, with a resolution of 0.1 degree crank angle.

2.4. Fast Heat Release

The logarithmic P-V diagram provides a good representation of engine work but cannot infer details of the combustion process to directly relate the pressure rise due to the chemical energy released. While detailed heat release analysis based on the first law of thermodynamics includes subroutines for estimating burned gas properties with chemical equilibrium and prediction of the trapped residual mass, these subroutines are time consuming and inapplicable for online diagnostic purposes. Alternatively, a simplified fast heat release method that has been widely applied [2] is used here. The fast heat release analysis is based on the assumption of a single zone combustion chamber and a fixed ratio of specific heats for gas properties.

The energy equation based on the 1st law of thermodynamics can be expressed as follows for a closed system to evaluate its efficiency during high CV conditions:

$$\frac{dQ_{ch}}{d\theta} = \frac{m_c c_v dT}{d\theta} + P\frac{dV}{d\theta} + \frac{dQ_{ht}}{d\theta}, \tag{7}$$

based on the assumption of ideal gas law :

$$PV = m\frac{\overline{R}}{M}T. \tag{8}$$

Introducing the differential from the ideal gas law into the energy equation yields:

$$\frac{dQ_n}{d\theta} = \frac{dQ_{ch}}{d\theta} - \frac{dQ_{ht}}{d\theta} = \frac{\gamma}{\gamma-1}P\frac{dV}{d\theta} + \frac{1}{\gamma-1}V\frac{dP}{d\theta}. \tag{9}$$

The apparent heat release is calculated by solving Eq. 9 while gamma is assumed to be constant (1.35). Eq. 9 was evaluated from the start to end of combustion (SOC and EOC respectively) to determine the net rate of heat release. SOC was defined as the crank angle of intake valve closing (IVC) for HCCI and the crank angle of spark for SI. EOC was defined as 30 degrees after top dead center, where combustion ends in most cycles. The mass fraction burned (x_b) was defined by normalizing the cumulative heat release from SOC to a given crank angle by the net cumulative heat release determined from SOC to EOC. The corresponding combustion phasing is then defined proportional to the mass fraction burned. The initial condition of pressure and volume for each cycle is defined slightly before the SOC from the experimental pressure measurement. Although the residual mass is not considered in this case, the initial condition is updated each cycle to reflect the variation of in-cylinder charge.The coupled equations and their convergence has been studied for a HCCI application in our previous work [11]

While the choice of EOC affects the combustion phasing calculation (CA50), this choice did not affect the HCCI and SI symbol statistics for slow burning or misfiring cycles, or the quantification of random or deterministic patterns discussed in the next Section. Due to the equally probable coarse binning approach, this approach lumps very slow burning and misfiring cycles into a single bin.

Applying the three methods on pressure data from SI combustion, the CA50 calculated from each method is shown in Fig. 3. It is shown in Fig. 3(a) and (b) that all the three fast computation methods perform well for SI combustion with small discrepancies relative to the baseline detailed heat release analysis, labeled as dHR. The CA50 calculation for HCCI combustion is shown in Fig. 4. Deviations from baseline are observed for all of the three fast computation methods. However, the inaccuracies of these three methods in the estimation of SI combustion phasing were found mostly for slow burning cycles. CA50 computations were performed on a 2GHz Intel Core i7 with 8GB Memory, with calculation times (per cycle) within 10 ms for the three methods.

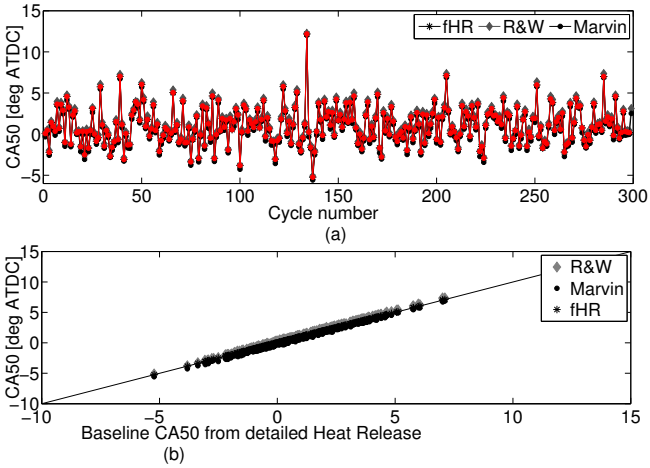

Figure 3. CA50 calculation of SI combustion with 42% internal EGR fraction, spark timing 38 deg bTDC (a) Scatter plot (b) Relationship with the baseline CA50 from detailed heat release. Detailed heat release is noted as dHR and fast Heat Release is noted as fHR. Marvin's method is noted as Marvin and Rasseweiler and Withrow's method is noted as R&W

In summary, the fast heat release and Rasseweiler and Withrow's methods are accurate for rapid burning HCCI combustion cycles but could result in discrepancies in late burning cycles. This is due to the fact that both methods involve an arbitrarily defined end of combustion, which contributes to most of the inaccuracy in phasing estimations for the late burning cycles. Marvin's method could result in noticeable deviation due to the constant

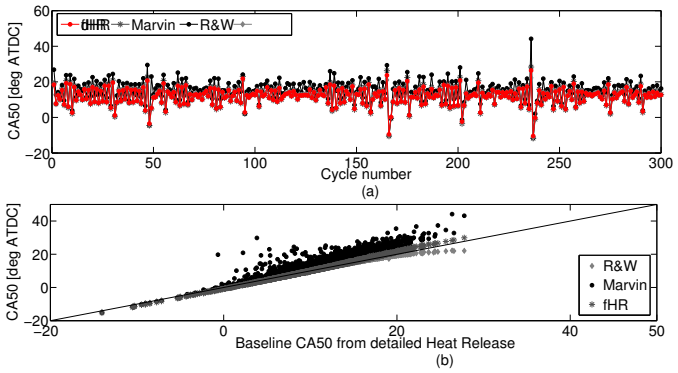

Figure 4. CA50 calculation of HCCI combustion. (a) Scatter plot (b) Relationship with the baseline CA50 from detailed heat release

volume assumption and limited resolution when determining the intersection point.

3. Determinism versus Randomness in Cyclic Variation

The cyclic dispersion of SI and HCCI combustion were quantified with return maps, modified Shannon Entropies and symbol sequence statistics [9] of the estimated combustion phasing parameters. These techniques help to quantify the influence of deterministic patterns in the seemingly random events. A brief summary of the three techniques is included for clarification purposes. A detailed description of these techniques can be found in references [3]. In this section, we investigate if the skewness of the fast methods described earlier could also affect the entropy of the combustion phasing for both deterministic HCCI and random SI combustion.

A return map qualitatively shows the relationship of two consecutive cycles of a specific cycle-dependent combustion feature. The modified Shannon entropy [3] is a quantitative measurement of the randomness of a given time series sequence. It shows the temporal correlation in time series data when discretised into symbols with a specific sequence division N and length L and is defined as:

$$H_s = -\frac{1}{logn_{seq}} \sum_k p_k log p_k, \tag{10}$$

where, p_k is the probability of observing a sequence k, and n_{seq} is the number of different sequences observed in the time series. the entropy equaling 1 ($Hs = 1$) represents a random process while $H_s < 1$ shows the presence of deterministic patterns. In practice, the modified Shannon entropy can be used to: (a) quantify the randomness in time series data and (b) optimize symbol sequence parameters N and L, with the best representation of temporal correlation occurring in the engine cycles. The symbol sequence histogram describes the probability of the occurrence of a specific sequence and hence could point to a deterministic mechanism causing this sequence.

3.1. Impact of Combustion Phasing Estimation on the Deterministic Patterns

To examine the impact of the combustion phasing estimation on quantifying deterministic patterns, we used previously published HCCI data [9]. The CA50 of HCCI combustion has been used to examine the sensitivity of the quantification of cyclic variation to processing method. Fig. 5 is the return map of CA50 calculated from various fast methods superimposed onto the baseline CA50 calculated with the detailed heat release. Oscillations between early and later cycles are observed, representing the presence of non-randomness for each of the three fast computation methods. The fast heat release and Rasseweiler and Withrow's method had negligible impact on the return map, while Marvin's method distorts the map slightly.

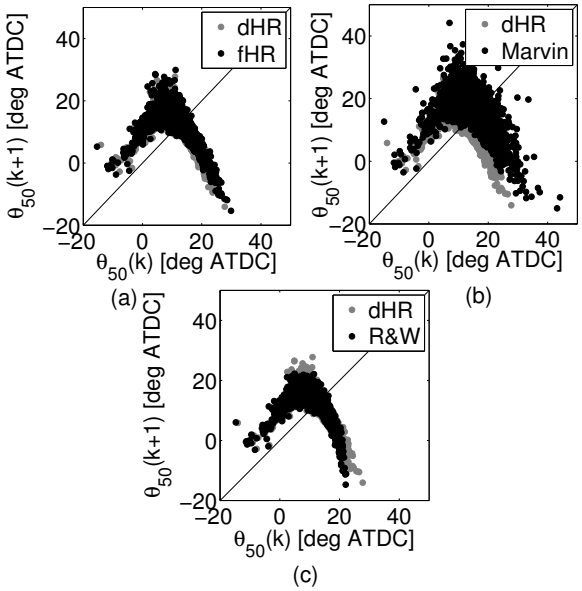

Figure 5. Return map of CA50 of high cyclic variation HCCI combustion. (a) Detailed Heat Release (noted as dHR in grey dots) v.s. fast Heat Release (noted as fHR, in black dots) (b) Detailed Heat Release (noted as dHR in grey dots) v.s. Marvin's method (noted as Marvin, in black dots) (c) Detailed Heat Release (noted as dHR in grey dots) v.s. Rasseweiler and Withrow's method (noted as R&W, in black dots)

The modified Shannon entropy of CA50 from detailed heat

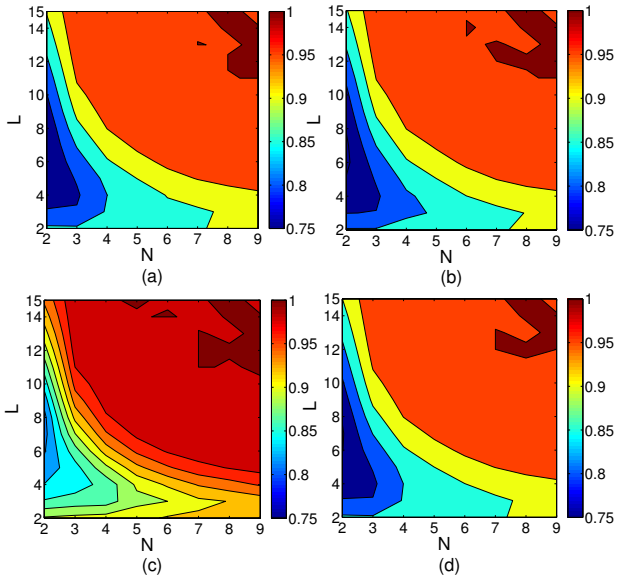

Figure 6. The modified Shannon entropy of CA50 of high cyclic variation HCCI combustion. (a) Detailed Heat Release (b) Fast Heat Release (c) Marvin's method (d) Rasseweiler and Withrow's method

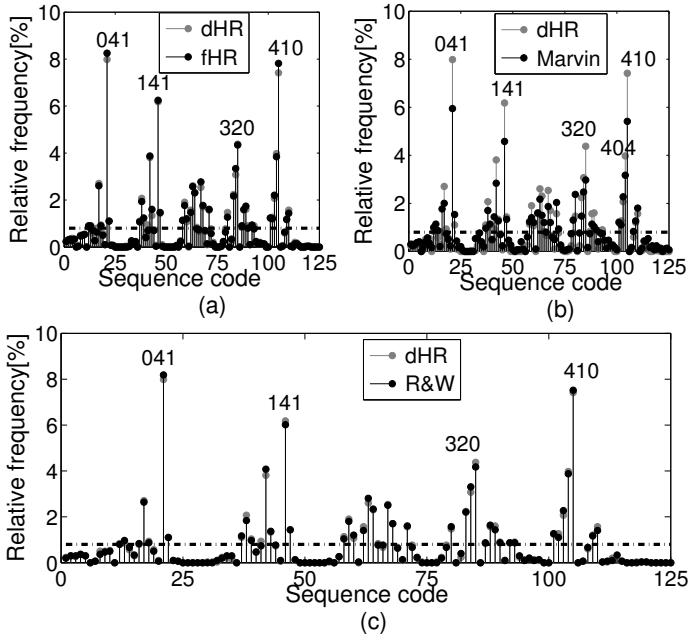

Figure 7. Symbol statistics of CA50 of high cyclic variation HCCI combustion. (a) Detailed Heat Release v.s. Fast Heat Release (b) Detailed Heat Release v.s. Marvin's method (c) Detailed Heat Release v.s. Rasseweiler and Withrow's method

release is shown in Fig. 6(a) as the baseline, with the fast heat release, Marvin's method, Rasseweiler and Withrow's method shown in (b), (c) and (d), respectively. The minimum Shannon Entropy of the baseline case is around 0.75, with each of the three fast processing methods resulting in a similar value, suggests that the deterministic dynamic behaviour could be captured by either method. However, Marvin's method shows a decrease in the magnitude in the modified Shannon entropy with various combinations of partition number N and sequence length L, consistent with the deviation observed in the return maps in Fig. 5.

The symbol statistics of CA50 are shown in Fig. 7 for the three fast computation method with baseline detailed heat release plotted in grey. Sequence partition number N and sequence length L are defined as 5 and 3, consistent with the approach of our previous work [12]. Such combination yields a magnitude of 0.85 for the modified Shannon entropy, but it is not the lowest value for all of the combinations. Any of the three methods captures certain sequences (for example 041, 410, 141, 320) with higher frequency, which suggests the undergoing deterministic dynamics induced by the recirculated residual gas [9]. Despite the discrepancies in estimating CA50 with Marvin's method, the sequences are identified in symbol statistics, Fig. 7(b). This is due to the coarse binning approach of symbol sequencing that ensures the robustness of this quantification technique.

The return map, modified Shannon entropy and symbol statistics for 298 cycles at the condition with highest internal EGR rate are plotted in Fig. 8. The scatter-ball-shaped return map in Fig. 8(a) qualitatively indicates randomness. The contour of the modified Shannon entropy of CA50 with sequence division $N(N = 2,3,9)$ and length $L(L = 2,3,15)$ is shown in Fig. 8(b), with the minimum magnitude of the modified Shannon entropy around 0.975 which quantitatively shows the combustion phasing of SI combustion to be random. There are no sequences with relative high frequency in the symbol statistics shown in Fig. 8(c). Thus, in the SI case presented here, we observe randomly distributed patterns in the cyclic variations. This conclusion is obviously reached for all the methods of computing the CA50, since the variability in SI data we observed did not include slow burns and late combustion.

4. Diagnostic of Determinism

To decide if SI and HCCI combustion is deterministic or random and to select the corresponding control strategy, we introduce a diagnostic technique based on the permutation entropy [13, 14], which quantifies the rank order pattern of combustion phasing and tracks the temporal development of 'determinism' in the time series data. Comparisons with the modified Shannon entropy are made as follows. The theory of permutation is

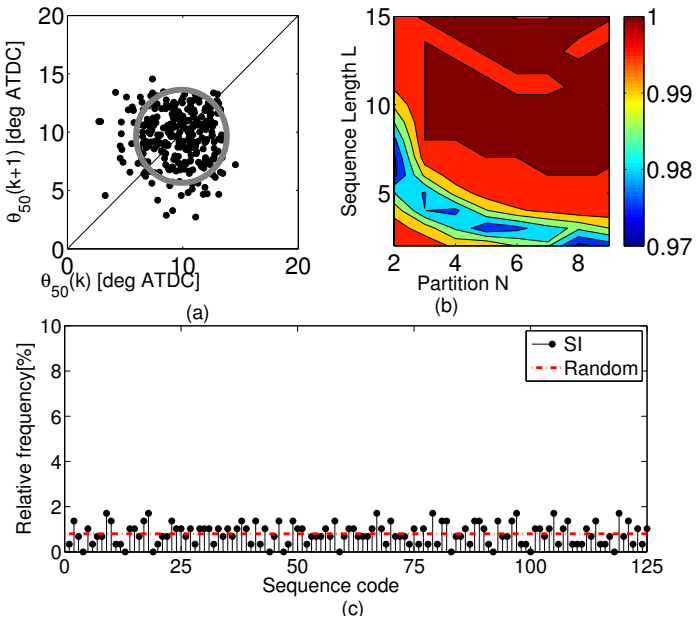

Figure 8. Quantification of cyclic variation in SI combustion with 42% internal EGR fraction, spark timing 38 deg bTDC (a) Return map (b) The modified Shannon entropy (c) Symbol statistics

briefly described before discussing an application to HCCI and SI combustion.

4.1. Permutation Entropy

The permutation entropy is an invariant of the rank order pattern in time series data proposed by Bandt and Pompe [13] based on entropy measures and symbolic dynamics. It has been applied to quantify combustion complexity, flame front dynamics [15] and to detect blowout in a lean burn premixed gas-turbine [16]. Symbol statistics rely on coarse binning with the benefit of robustness in the presence of noise. However, this robustness sacrifices the large volume of information contained in the re-representation of the time series data. In order to capture more details, larger partition numbers N and sequence lengths L are needed, but this would result in large number of combinations N^L and would cause difficulties in identifying specific sequences with relatively higher frequency above the random line. Permutation is based on sorting and could provide additional information and work together with Shannon entropy and symbol statistics to examine if the time series data is deterministic or random.

Permutation entropy of the time series data could provide tracking of rank order patterns. Given a time series $X = x_i, i = 1,...,m$ with m as the number of time series data, the chosen order of permutation n defines the dimension in phase space. For example, an order of permutation $n = 4$ defines a three-dimensional phase space and quantifies the rank order pattern of $x_i, x_{i+\tau}, x_{i+2\tau}, x_{i+3\tau}$. The relative frequency of each permutation is calculated as:

$$p_j = \frac{z_j}{\sum z_k}, \tag{11}$$

where z_j is the count of realisation of the jth permutation and z_k is the total realisations. Following the definition of Shannon entropy, the permutation entropy is defined as:

$$H_p = -\sum_{j=1}^{n!} p_j log_2(p_j). \tag{12}$$

The permutation entropy H_p is then normalised by the maximum permutation entropy $log_2 n!$ following Domen's approach [16] noted as H_n as in Eq. 13, so that $H_n = 0$ corresponds to a monotonic relationship that is completely deterministic and $H_n = 1$ corresponds to randomness.

$$H_n = \frac{-\sum_{j=1}^{n!} p_j log_2(p_j)}{log_2 n!}. \tag{13}$$

An graphic example of data discretization for the calculation of permutation entropy is given in Fig. 9. A detailed step by step description is provided in reference [14]. Comparing to binning discretization for the symbol statistics and the modified Shannon entropy, the discretization approach for permutation represents the ranking order value in data sequence. This is the major difference between the definition of the permutation entropy the modified Shannon entropy [3].

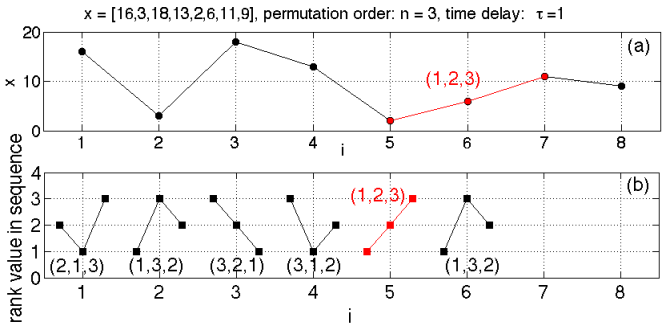

Figure 9. Example of discretization of the calculation of permutation entropy (a) Time series example (b) Rank order

4.2. Diagnostic of Determinism with Varying Operating Conditions

The modified Shannon entropy and the permutation entropy of CA50 of HCCI and multi-cylinder SI combustion were calculated. These analyses are now extended to handle variations in engine operating conditions, which will be encountered given the transient nature of engine applications. The CA50 values are calculated from in-cylinder pressure with the three fast computational methods as well as the baseline detailed heat release analysis. The influence of the three fast computational methods on entropies is examined.

For each of the four cylinders, 298 cycles of CA50 of a SI combustion engine are arranged by the firing order 1-3-4-2. To represent the entropy characterisation of both random and deterministic data, 3,000 cycles of HCCI CA50 are shown as a reference. The normalised permutation entropy H_n and the modified Shannon entropy with partition $N = 4$, $L = 3$ of CA50 of HCCI and SI combustion is shown in Fig. 11(c). The order of permutation entropy n is chosen as 4. The time delay τ is chosen as 1 and window size $\hat{m}$ as 100. The procedure of calculating Shannon Entropy is summarized below with 3000 cycles of HCCI data as an example. The same procedure applies to the permutation entropy.

Step 1. Define the window of interest with size of $\hat{m}$ that contains $X = x_i, i = 1, ..., \hat{m}$ cycles. For $\hat{m}$ = 100, 100 cycles are used to calculate the Shannon Entropy H_s.
Step 2. Slide the window of interest with a step of 1 cycle and repeat Step 1 until cycle $x_{m-\hat{m}}$.

The window size $\hat{m}$ should be chosen considering the cycles required for the entropy to converge and will be studied in our future work.

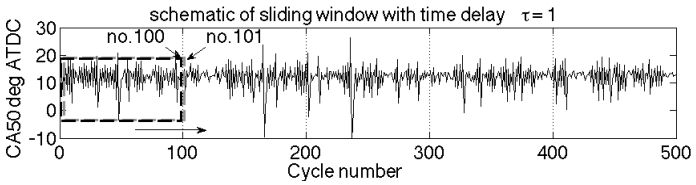

Figure 10. Schematic of the sliding window used to enable entropy calculations with varying operating conditions.

A graphic schematic of the sliding window method used to enable entropy calculation with varying operating conditions is shown in Fig. 10.

A scatter plot of the CA50 of HCCI and SI combustion calculated with detailed heat release analysis is shown in Fig. 11(a) with HCCI data shown in black and SI data shown in grey. The difference in CA50 magnitude reflects the mean value difference without indication on determinism or randomness nature. Fig. 11(b) provides quantification on the deviation from the COV of IMEP and standard deviation of CA50, which are calculated within 100 cycles and move at the time lag of 1 cycle. SI combustion shows less deviation from the value calculated over the entire range of sampling cycles while HCCI combustion displays more intense fluctuations. Also, the standard deviation of CA50 and COV of IMEP correlate well. The entropy values deviate from one, suggesting the data to be deterministic in the HCCI region and approach one in the random SI region.

It should be mentioned that a discontinuity is observed in the temporal evolution of variations and entropies from around 2,900 to 3,000 for HCCI and after around 4,100 for SI. The Discontinuity range is determined by the chosen window size, which is 100 in the current result shown in Fig. 11. This is due to the artificially stitched HCCI and SI data, which does not represent a real experiment with observed abrupt switching between two combustion modes.

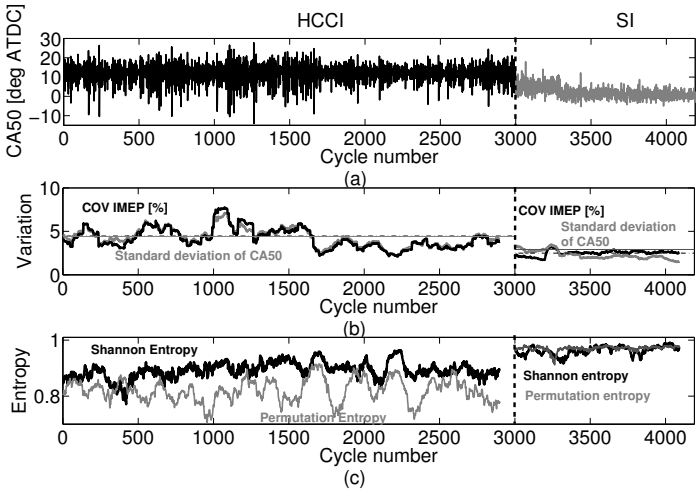

Figure 11. Diagnostic of determinism in HCCI and SI combustion. (a) Scatter plot of CA50 of HCCI and SI combustion (b) COV of IMEP and standard deviation of CA50 for 100 cycles with step of 1 (c) The modified Shannon entropy and the permutation entropy for 100 cycles with step of 1 cycle, the permutation order is 4.

The influence of the three fast computational methods on entropy tracking is examined as follows. The permutation entropy and the modified Shannon entropy described above are calculated for CA50 from the three fast computational methods. Unlike Fig. 11(b) and (c), that the entropy evolutions are calculated separately for the HCCI and SI cycles, Fig. 12 shows calculations for the evolution of the entropies for artificially constructed

3,000 cycles of HCCI connected by 298 $\times$ 4 cycles of SI combustion. This is to examine the entropy response to a known changed magnitude of determinism in the time series data. The permutation entropy is shown in Fig. 12(a) and the modified Shannon entropy is shown in Fig. 12(b).

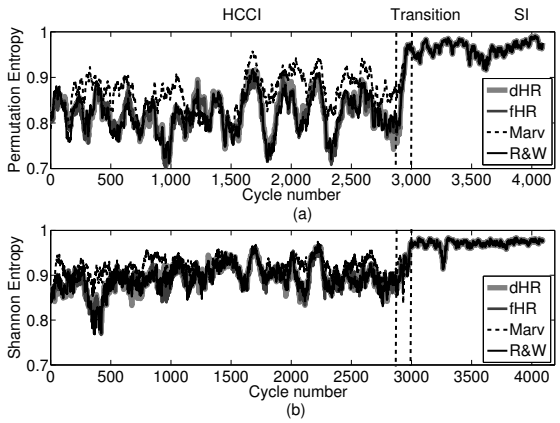

Figure 12. Diagnostic of determinism in HCCI and SI combustion. (a) Permutation entropy (b) Shannon Entropy. Note: 2,999 cycles of HCCI combustion and 1,192 cycles of SI combustion are artificially joined together for this analysis, which is intended to demonstrate the entropy's response to a change in operating conditions with no real experiment with combustion mode switch.

For both permutation entropy and the modified Shannon entropy, the entropy evolutions of CA50 from fast heat release and Rasseweiler and Withrow's Method agree well with the baseline CA50 from detailed heat release. Marvin's method could result in an increase in both entropies, suggesting a decrease in the quantified determinism, consistent with the results of symbol statistics. Thus Marvin's method should be avoided in the studies of cyclic variation.

To show the entropy response to a known changed magnitude of determinism in time series data, Fig. 12 is magnified between cycle 2,900 to 3,000 shown in Fig. 13. Both entropies gradually increase from lower values of deterministic HCCI to higher values of random SI cycles.

To further examine the response of the two entropies, the first derivative and its cumulative value of the permutation entropy and Shannon entropy during the transition cycle 2,900 to 3,00 as shown in Fig. 14. Both entropies respond fast to the switch. The difference is the magnitude of the permutation entropy is lower than the Shannon entropy, which might be advantageous when determining the threshold shown in Fig. 15 during the selection of the corresponding control strategy.

The entropy diagnostic method could assist the selection of the corresponding control strategy. This process is illustrated as a

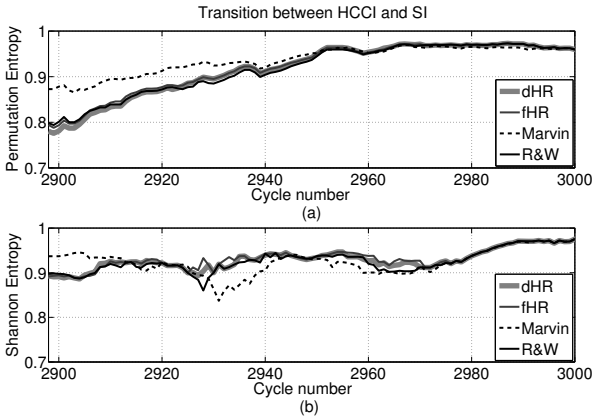

Figure 13. Diagnostic of determinism in HCCI and SI combustion between HCCI and SI transition. (a) Permutation entropy (b) Shannon Entropy. Note: 2,999 cycles of HCCI combustion and 1,192 cycles of SI combustion are artificially joined together for this analysis, which is intended to demonstrate the entropy's response to a change in operating conditions with no real experiment with combustion mode switch

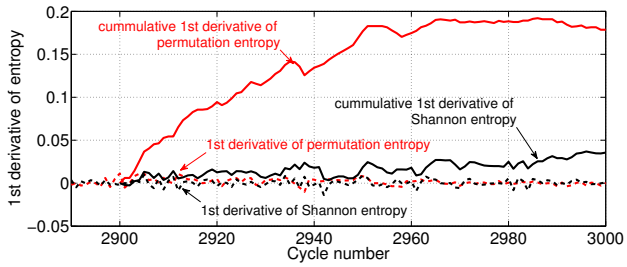

Figure 14. The 1st derivative of permutation entropy and Shannon entropy with combustion phasing calculated from detailed heat release analysis. Note: 2,999 cycles of HCCI combustion and 1,192 cycles of SI combustion are artificially joined together for this analysis, which is intended to demonstrate the entropy's response to a change in operating conditions with no real experiment with combustion mode switch.

diagram in Fig.15. In the case of high CV with underlying deterministic patterns, it is possible to apply closed loop combustion control on a cyclic-basis with a fixed mean value, such as injection timing in HCCI or spark timing in SI, to contract the CV. In the case of a random distribution, the high CV can be avoided by shifting operating conditions away from the unstable region. It should be noted that the threshold for both entropies will possibly need calibration. We intend to examine the threshold online on an engine dyno and present more results in our future publications. The determination of the value of the thresholds requires more thorough investigations and is beyond the current scope of this paper.

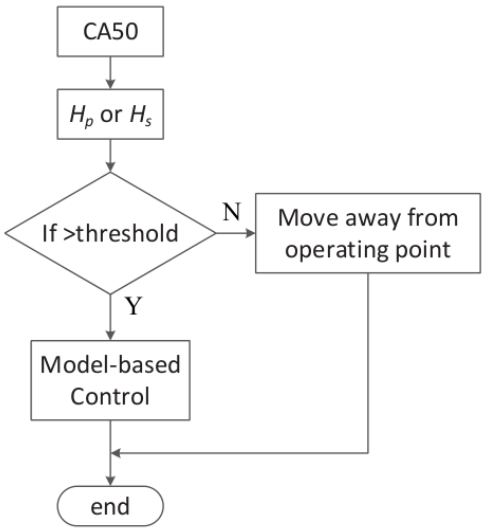

Figure 15. Block diagram of selection of control strategy

Conclusion

In summary, the current work has evaluated the affect that various fast CA50 calculation methods have on the quantification of CV as either random or deterministic. We have found that combustion phasing derived from the single zone fast heat release and the Rasseweiler and Withrow's method had negligible impact when quantifying deterministic patterns, however Marvin's method could cause certain deviations in the deterministic patterns that one should be aware of when quantifying cyclic variation. The robustness in quantifying the cyclic variability with on-board combustion phasing estimation indicates the potential for short-term online feedback control.

We have used an diagnostic method to quantify the deterministic and random nature of SI and HCCI combustion based the permutation entropy, with its performance compared to modified Shannon entropy [3].

Combustion phasing derived from the single zone fast heat release and the Rasseweiler and Withrow's method had negligible impact on the entropy tracking algorithms. However, the combustion phasing calculated from Marvin's method could increase both the permutation and the modified Shannon entropy, resulting in misinterpretation of the determinism of time series data.

Parameterisation for the modified Shannon Entropy and the permutation entropy is one of the interesting directions of future works that would extend the application of this quantification technique.

ACKNOWLEDGMENT

The authors would like to thank Dr. Shyam Jade for the SI data and Dr. Eric Hellström's correspondence for useful discussions.

REFERENCES

[1] Nüesch, S., E. Hellström, L. J., and Stefanopoulou, A., 2014. "Mode switches among si, saci, and hcci combustion and their influence on drive cycle fuel economy". *in Proceedings of American Control Conference (ACC) 4-6 June 2014*, pp. 849–854.

[2] Heywood, J., 1988. *Internal Combustion Engine Fundamentals*, 1st ed. McGraw-Hill Science/Engineering/Math.

[3] Wagner, R., Edwards, K., Daw, C., Green, J., and Bunting, B., 2006. "On the nature of cyclic dispersion in spark assisted hcci combustion". *SAE Technical Paper,* **2006-01-0418**.

[4] Sen, A., Litak, G., Edwards, K., Finney, C., Daw, C., and Wagner, R., 2011. "Characteristics of cyclic heat release variability in the transition from spark ignition to hcci in a gasoline engine". *Applied Engergy,* **88**, pp. 1649–1655.

[5] Larimore, J., Jade, S., Hellström, E., Stefanopoulou, A., Vanier, J., and Jiang, L., 2013. "Online adaptive residual mass estimation in a multicylinder recompression hcci engine". *ASME 2013 Dynamic Systems and Control Conference (DSCC),* **3**.

[6] Marvin, C., 1927. "Combustion time in the engine cylinder and its effect on engine performance". *NACA Report No.276*.

[7] Prakash, N., Martz, J., and Stefanopoulou, A., 2015. "A phenomenological model for predicting combustion phasing and variability of spark assisted compression ignition (saci) engines". *ASME 2015 Dynamic Systems and Control Conference, Columbus, OH, USA, October 28 - 30*.

[8] Hellström, E., Stefanopoulou, A., and Jiang, L., 2013. "A linear least-squares algorithm for double-wiebe functions applied to spark-assisted compression ignition". *Journal of Engineering for Gas Turbines and Power,* **136**.

[9] Hellström, E., Larimore, J., Stefanopoulou, A., Sterniak, J., and Jiang, L., 2012. "Quantifying cyclic variability in a multi-cylinder hcci engine with high residuals". *In Proceedings of the ASME 2012 Internal Combustion Engine Division Spring Technical Conference, Torino, 6–9 May 2012*.

[10] Rassweiler, G., and Withrow, L., 1938. "Motion pictures of engine flame correlated with pressure cards". *SAE Journal (Trans),* **42**, pp. 185 – 204.

[11] Larimore, J., Hellström, E., Jade, S., Stefanopoulou, A., and Jiang, L., 2014. "Real-time internal residual mass estimation for combustion with high cyclic variability". *Inter-*

national Journal of Engine Research, **Cyclic Dispersion Special Issue**.

[12] Hellström, E., Larimore, J., Jade, S., Stefanopoulou, A., and Jiang, L., 2014. "Reducing cyclic variability while regulating combustion phasing in a four-cylinder hcci engine". *IEEE Transactions on Control Systems,* **22**, pp. 1190–1197.

[13] Bandt, C., and Pompe, B., 2002. "Permutation entropy: a natural complexity measure for time series". *Physical Review Letters,* **88**, p. 174102.

[14] Riedl, M., Muller, A., and Wessel, N., 2013. "Practical considerations of permutation entropy". *The European Physical Journal - Special Topics,* **222**, pp. 249–262.

[15] Gotoda, H., Michigami, K., Ikeda, K., and Miyano, T., 2010. "Chaotic oscillation in diffusion flame induced by radiative heat loss". *Combustion Theory and Modelling,* **14**, pp. 479–493.

[16] Domen, S., Gotoda, H., Kuriyama, T., Okuno, Y., and Tachibana, S., 2015. "Detection and prevention of blowout in a lean premixed gas-turbine model combustor using the concept of dynamical system theory". *Proceedings of the Combustion Institute,* **35**, pp. 3245–3253.